

Effect of vitrification on mechanical properties of porcine articular cartilage

Proc IMechE Part H:
J Engineering in Medicine
2022, Vol. 236(10) 1521–1527
© IMechE 2022



Article reuse guidelines:

sagepub.com/journals-permissions

DOI: 10.1177/09544119221122066

journals.sagepub.com/home/pih



Jenny He¹, Itai Wine², Kezhou Wu^{1,3}, Johnathan Sevick¹, Leila Laouar¹,
Nadr M Jomha¹ and Lindsey Westover⁴

Abstract

Articular cartilage (AC) injuries do not heal primarily and large lesions progress to degenerative osteoarthritis. Osteochondral allograft transplantation is an effective surgical treatment but is limited by the lack of donor tissue availability. Fresh allografts can be stored hypothermally up to 28–45 days after which the tissue is no longer viable for transplantation. Vitrification is a method of cryopreservation with the potential to extend the storage time of AC. A specific protocol has been demonstrated to preserve high chondrocyte viability; however, its effect on various mechanical properties of the extracellular matrix (ECM) remains unknown and is the focus of this initial study. Porcine AC was subject to a defined vitrification protocol, using fresh and frozen samples as positive and negative controls, respectively; $n = 20$ for all three groups. Unconfined compression testing was used to assess mechanical properties of the tissue under rapid load, stress relaxation, and equilibrium conditions. The stress relaxation time constants (modeled with a 2-term Prony series) τ_1 and τ_2 were significantly lower for frozen ($p = 0.014$, $p < 0.001$) and vitrified ($p = 0.009$, $p = 0.003$) tissue compared to fresh, with no differences between frozen and vitrified samples ($p = 0.848$ and 0.105 for τ_1 and τ_2 , respectively). These values indicate that frozen and vitrified samples relaxed more rapidly than fresh, which may suggest altered matrix composition and permeability post-treatment. These results represent the initial study in our experimental path to evaluate differences in mechanical properties of vitrified tissues.

Keywords

Articular cartilage, vitrification, mechanical properties, arthritis, transplantation

Date received: 29 September 2021; accepted: 8 August 2022

Introduction

Articular cartilage (AC) lesions in the knee are common, particularly in young and active patients. Due to its avascular nature, AC injuries do not heal independently and often progress to osteoarthritis.¹ Osteochondral (bone and AC) transplantation has become an established surgical treatment for focal AC defects that restores function and can prevent/delay the need for arthrodesis/arthroplasty. Allografting of fresh osteochondral tissue to treat focal femoral condyle lesions has documented long-term success rates between 70% and 90% at 12 years.² The success of this surgery has made it increasingly popular but availability and cost of donor tissue remain the most significant limitations.³

Currently, allografts are harvested within 24 h of donor death and must undergo a regulatory screening process for contamination and disease which requires

approximately 14 days.^{4,5} Fresh grafts are stored at 4°C while matching for size, contour, and exact location with potential recipients. After 28–45 days of storage, they must be discarded.^{6,7} Fresh grafts are preferred over frozen grafts (stored at -80°C) because they have higher chondrocyte viability,⁷ improved cartilage

¹Department of Surgery, University of Alberta, Edmonton, AB, Canada

²Department of Civil and Environmental Engineering, University of Alberta, Edmonton, AB, Canada

³Department of Orthopedic Surgery, First Affiliated Hospital, Shantou University Medical College, Shantou, Guangdong, China

⁴Department of Mechanical Engineering, University of Alberta, Edmonton, AB, Canada

Corresponding author:

Lindsey Westover, Department of Mechanical Engineering, University of Alberta, 9211 116 Street NW, 10-371 D-ICE Building, Edmonton, AB T6G 1H9, Canada.

Email: lwestove@ualberta.ca

stiffness, increased matrix content and decreased surface degeneration 6 months after implantation,⁸ but are limited by finite storage time.

Vitrification, a form of cryopreservation that uses a high concentration of cryoprotective agents (CPAs) to prevent the formation of ice crystals,⁹ has been proposed as a means of prolonging allograft storage time without excessively sacrificing chondrocyte viability.¹⁰ The ability to store AC indefinitely would increase the availability of donor tissue, but the effect of vitrification on tissue mechanical properties has yet to be documented.

Graft survival depends on both chondrocyte and ECM integrity since the cellular component is required for long-term ECM function.¹¹ Therefore, cryopreservation must attempt to preserve both. Freezing protocols have been shown to cause damage to both cellular and extracellular components, possibly due to ice crystal formation during the freeze-thaw process.^{12–14} Freezing also affects various mechanical properties of AC, including decreasing aggregate modulus and half-life of stress-relaxation¹⁵; as well as decreasing stiffness and peak stress.¹⁶ Vitrification can maintain cell viability,¹⁰ so the objective of this preliminary study was to compare the mechanical properties of fresh, frozen, and vitrified porcine AC, and to guide further investigation. Because vitrification eliminates the formation of ice crystals, we hypothesized that vitrified AC will retain similar mechanical properties to fresh AC and superior mechanical properties compared to frozen AC. This outcome would support the use of vitrification for storing osteochondral tissue samples before transplantation.

Methods

Specimen harvest and preparation

Twenty femoral condyles were harvested from sexually mature porcine hind stifle joints obtained from pigs used for meat consumption from a local deli within 24 h of death. No animals were specially sacrificed for this project. The use of animal tissue for research was approved by the Research Ethics Office at the University of Alberta. These joints were submerged in phosphate-buffered saline (PBS). Three 10 mm diameter osteochondral dowels (OCDs) were cored from each condyle using a handheld coring device. All three OCDs from a single condyle were transferred to the same beaker and cleaned with sterile PBS supplemented with antibiotics (100 units/mL penicillin, 100 µg/mL streptomycin, 0.25 µg/mL amphotericin B) under a sterile biosafety cabinet for 20 min. The OCDs were then placed in Falcon tubes containing 25 mL of sterile Dulbecco's Modified Eagle Media (DMEM) complete medium [(DMEM complete: Dulbecco's Modified Eagle Medium F12 (Gibco) supplemented with 10% Newborn Calf Serum (Gibco), 100 units/mL penicillin, 100 µg/mL streptomycin, 0.25 µg/mL amphotericin B

(Gibco), and 1 mM sodium pyruvate (Gibco)] and stored at 4°C overnight. The three OCDs from each condyle were randomly assigned to one of three experimental groups (fresh, frozen, and vitrified) using a paired design ($n = 20$ per group).

Fresh

OCDs in the Fresh Group were kept in DMEM complete at 4°C for approximately 40 h until mechanical testing.

Frozen

OCDs in the Frozen Group were kept in DMEM complete at 4°C overnight, then transferred to PBS and subjected to four freeze-thaw cycles by plunging into liquid nitrogen (LN₂) at -195.79°C for 15 min and warming to 37°C using a water bath.

Vitrified

OCDs in the Vitrified Group were kept in DMEM complete at 4°C overnight, then underwent vitrification the following day. The 7-h vitrification process, briefly summarized here, involved the use of several CPAs at increasing concentrations and progressively lower temperatures, followed by rapidly plunging in LN₂ and held overnight.¹⁷ All solutions were made in DMEM.

Solution 1: 3 M dimethyl sulfoxide (DMSO) + 3 M ethylene glycerol (EG) at 0°C for 90 min

Solution 2: 3 M DMSO + 3 M EG + 3 M propylene glycerol (PG) at -5°C for 170 min

Solution 3: 3 M DMSO + 3 M EG + 2 M PG at -10°C for 160 min

After warming to 37°C using a water bath, samples were washed with agitation on an orbital shaker at 180 rpm for 30 min in 25 mL of DMEM at 4°C.

Mechanical testing

Prior to mechanical testing, all OCDs were warmed to room temperature and rehydrated in PBS for 1.5 h. Cartilage was removed from the bony base of the dowel using a surgical blade. Cartilage thickness was measured using a digital caliper at three locations per sample to determine an average initial thickness. When possible, samples were re-punched using the 10 mm diameter core to ensure cross-sectional consistency and to eliminate the effect of the initial coring angle on the samples' shapes. The cross-sectional area was calculated by taking a photograph of each OCD and analyzing it in a custom MATLAB image processing algorithm to ensure consistency across samples and to determine an accurate cross-sectional area for use in calculations. The software was calibrated using a reference ruler (see Figure 1). Samples were then placed on a non-porous

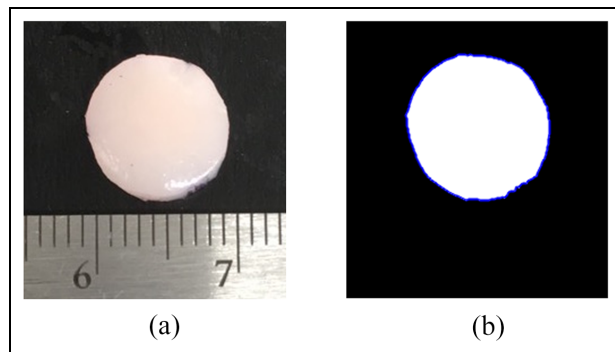


Figure 1. (a) Example image of an OCD with a reference ruler used for calibration and (b) an image processing MATLAB algorithm using the reference ruler, and the tracked edge of the OCD (blue) to calculate the cross-sectional area.

steel disc, within a room temperature PBS bath, for uniaxial unconfined compression testing using the Bose ElectroForce 3200. They were compressed from the top using a non-porous steel disc. The following loading protocol was used: (1) 1 N pre-load held for 120 s, (2) rapid loading at a strain rate of 15%/s to 15% strain, (3) displacement held for at least 1800 s to allow stress-relaxation to an equilibrium state.

Data analysis

AC was assumed to act as an incompressible material under the applied rapid loading rate.¹⁸ The stress-strain behavior in the rapid loading phase was modeled using a Mooney-Rivlin material model, where constants C_1 and C_2 in the following equation were determined:

$$\sigma = (2C_1 + 2C_2/\lambda)(\lambda^2 - 1/\lambda)$$

Where σ is the compressive stress and λ is the stretch ratio, defined as compressed thickness divided by initial thickness. Further, peak stress corresponding to the applied 15% strain was determined from the measured load. The secant modulus (E_s), representing apparent stiffness under rapid loading, was calculated as peak stress divided by applied strain (15%). In an assessment of several common hyperelastic models, the Mooney-

Rivlin formulation was suggested to provide the most capable representation of normal and degraded cartilage.¹⁹ The stress-relaxation behavior was modeled using a 2-term Prony series to investigate the relaxation time constants τ_1 and τ_2 .^{20,21}

$$\sigma(t) = \sum_{i=1}^2 \sigma_i e^{-t/\tau_i} + \sigma_\infty$$

Finally, Young's modulus of the solid matrix was determined from the equilibrium stress values of the curve-fitted 2-term Prony series model (σ_∞).^{22,23} Differences in the estimated material properties between the three groups were investigated with repeated measures ANOVAs ($\alpha = 0.05$). Significant effects were investigated with linear contrasts.

Results

Table 1 shows a summary of the mechanical properties for the fresh, frozen, and vitrified groups reported as average \pm standard deviation values. Additionally, the p -values for the repeated measures ANOVAs are shown in Table 1. Three samples (one from each group) were excluded from the analysis because the cartilage was damaged during the coring and bone removal process. Further, one additional frozen sample was excluded from the stress-relaxation and equilibrium analysis because of technical issues with the Bose ElectroForce 3200 during testing.

Rapid loading

Using the Mooney-Rivlin model for rapid loading, the average C_1 values were -2.09 , -2.07 , and -2.25 MPa for fresh, frozen, and vitrified respectively (Table 1). The average C_2 values were 2.23, 2.18, and 2.37 MPa for fresh, frozen, and vitrified respectively (Table 1). For both parameters, there were no significant differences between any of the three test groups, as C_1 values had an ANOVA p -value of 0.991, while C_2 had an ANOVA p -value of 0.983. It should be noted that the Mooney-Rivlin model provided an excellent representation of the experimental data with R^2 values above 0.99 for all samples.

Table 1. Summary of the mechanical properties in fresh, frozen, and vitrified AC samples (Average \pm SD; ANOVA p -values).

	Rapid Loading				Stress Relaxation		Equilibrium	
	C_1 (MPa)	C_2 (MPa)	Peak Stress (MPa)	Secant Modulus (MPa)	τ_1 (s)	τ_2 (s)	Equilibrium Stress (kPa)	Young's Modulus (kPa)
Fresh	-2.09 ± 1.48	2.23 ± 1.50	0.48 ± 0.26	3.19 ± 1.76	11.3 ± 3.5	145.9 ± 29.2	35.1 ± 16.8	234.1 ± 111.7
Frozen	-2.07 ± 1.18	2.18 ± 1.22	0.46 ± 0.22	3.07 ± 1.46	9.1 ± 4.3	113.1 ± 72.1	30.2 ± 12.4	201.4 ± 82.9
Vitrified	-2.25 ± 1.71	2.37 ± 1.77	0.48 ± 0.33	3.19 ± 2.19	8.3 ± 2.6	109.9 ± 24.1	27.2 ± 10.1	181.1 ± 67.1
ANOVA	0.991	0.983	0.883	0.883	0.023	0.094	0.305	

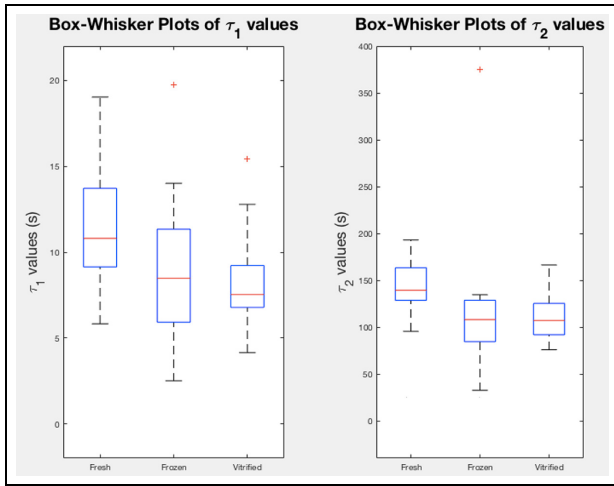


Figure 2. Box-whisker plots of τ_i values, which represent relaxation times. Outliers, which are identified by MATLAB as being more than 1.5 times the interquartile range away from the top or bottom of the box, are displayed by red “+”.

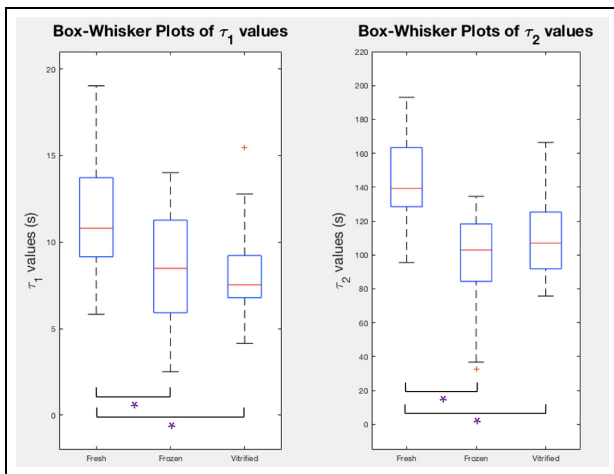


Figure 3. Box-whisker plots of τ_i values, which represent relaxation times. Outliers, which were identified by MATLAB, are not included in quartile calculations and are displayed by red “+”. Data sets separated by a “*” represent data sets that are significantly different ($p < 0.05$).

Peak stress and secant modulus

The average measured peak stress values were found to be 0.48, 0.46, and 0.48 MPa for fresh, frozen, and vitrified samples respectively (Table 1). The corresponding secant moduli were identified as 3.19, 3.07, and 3.19 MPa for fresh, frozen, and vitrified samples respectively. Again, there were no significant differences between any of the three test groups for these parameters ($p = 0.883$).

Stress-relaxation

Using the 2-term Prony series to model stress-relaxation, average τ_1 values were 11.3, 9.1, and 8.3 s for fresh,

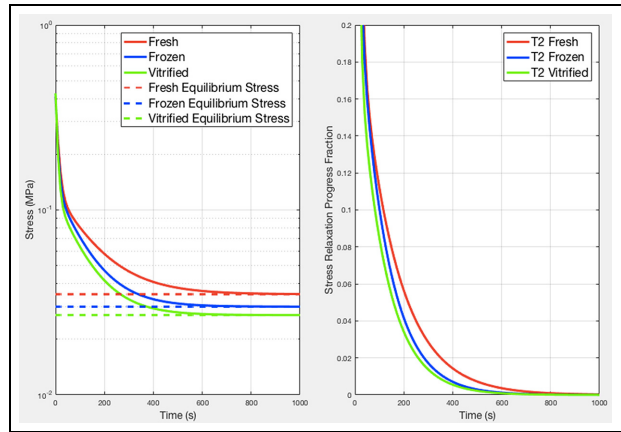


Figure 4. Left: general relaxation trends for each group of samples. Frozen and vitrified curves tend toward their equilibrium values quicker than the fresh curve, indicating a longer relaxation time for fresh samples. Right: progression of the average relaxation curves from peak stress (normalized to 1) to equilibrium stress, showing the percentage of stress from peak to relaxation.

frozen, and vitrified samples respectively (Table 1). The average τ_2 values were 145.9, 113.1, and 109.9 s for fresh, frozen, and vitrified samples respectively. The 2-term Prony series provided an excellent representation of the data with R^2 values greater than 0.99 for all samples. The ANOVA test indicated a significant difference between the groups for τ_1 ($p = 0.023$), while the differences were not significant for τ_2 ($p = 0.094$). Figure 2 shows a box plot for both the stress relaxation time constants where it was determined that one of the samples in the frozen group appeared to be an outlier for both τ_1 and τ_2 . The statistics were recalculated without this outlier with ANOVA p -values of 0.015 for τ_1 and < 0.001 for τ_2 . After removing the outlier, the average and standard deviation values for the frozen group were reduced to $\tau_1 = 8.5 \pm 3.5$ s and $\tau_2 = 97.7 \pm 31.4$. Linear contrasts revealed significant differences between fresh and frozen ($p = 0.014$ and $p < 0.001$ for τ_1 and τ_2 , respectively) and between fresh and vitrified ($p = 0.009$ and $p = 0.003$ for τ_1 and τ_2 , respectively), while there were no differences between the frozen and vitrified groups ($p = 0.848$ and $p = 0.105$ for τ_1 and τ_2 , respectively). Figure 3 shows the results for the stress-relaxation constants with the outlier removed, indicating the statistically significant differences. Figure 4 shows a representation of the stress relaxation curves using the average values for the fresh, frozen, and vitrified groups to visually represent the differences in relaxation parameters.

Equilibrium stress conditions

The average equilibrium stress values were 35.1, 30.2, and 27.2 kPa for fresh, frozen, and vitrified samples (Table 1). Young's modulus at equilibrium was determined to be 234.1, 201.4, and 181.1 kPa for fresh,

frozen, and vitrified samples. There were no significant differences between any of the three test groups for these parameters ($p = 0.305$).

Discussion

Osteochondral implantation using allograft tissue is an effective surgical treatment for joint defects, but its practical usage is restricted by limited storage options. Successful cryopreservation of AC would enable long-term storage which would alleviate this limitation. Chondrocyte viability and ECM integrity must both be maintained for successful transplantation.

Various attempts at cryopreservation have been shown to detrimentally affect chondrocyte viability,^{7,24} reducing or altering the capacity of the chondrocytes to maintain ECM components and leading to extensive graft tissue necrosis and fibrosis. Furthermore, changes in the ECM, such as those that occur with freezing, have been shown to disrupt the mechanical properties of AC.^{15,16} Ice crystal formation during the cryopreservation process has been proposed as a possible mechanism resulting in chondrocyte rupture and mechanical disruption of the extracellular collagen matrix and proteoglycan network, ultimately leading to graft failure.^{11,25} Physical damage resultant from ice crystal formation may include the breakdown of aggregating proteoglycans²⁶ and an increase in open areas in the matrix.²⁷ Four freeze-thaw cycles were employed to ensure all the chondrocytes within an intact cartilage sample were killed, which is based on previous work in our lab where at least three cycles in LN₂ consistently kills all of the cells.

Vitrification transitions a water-based solution into a glass-like solid without ice formation. Therefore, we hypothesized that it may preserve mechanical properties of the tissue. The vitrification protocol used employs stepwise cooling and multi-CPA solutions, which has been shown to mitigate CPA toxicity and maintain chondrocyte viability.¹⁰ However, it has not yet been shown in the literature what effect any vitrification protocol may have on AC mechanical properties.

Unconfined compression testing, as is commonly used in the literature to assess cartilage mechanics,^{22,28–30} was used to assess the effects of freezing and vitrification on the mechanical properties of porcine AC. No significant differences in mechanical parameters (secant modulus and Mooney-Rivlin material constants) between fresh, frozen, and vitrified samples were documented during the rapid loading phase. This result is partly consistent with the work of other research groups. Groups using indentation techniques to assess the unrelaxed (analogous to rapid loading phase of our study) and relaxed (analogous to equilibrium loading phase of our study) properties of cartilage have not found differences in either property between frozen or cryopreserved tissue and fresh tissue.³¹ Unconfined compression testing of bovine femoral condyle cartilage disks similarly produced

no detectable changes in biomechanical properties after a single freeze-thaw cycle to -20°C .³⁰ Black et al. also using indentation techniques, determined that the unrelaxed shear modulus of lapine femoral cartilage subjected to freeze-thaw was within the range of normal (i.e. fresh) and did not increase, unlike cartilage stored for increasing lengths of time.³²

In this study, the only significant difference was in stress-relaxation phase data between the three groups. A significant difference in the τ_i values was found between fresh and vitrified samples and between fresh and frozen samples. A 2-term Prony series was chosen for modeling stress-relaxation behavior over the 1 or 3 term series after assessing all three models with our data. Two terms most accurately represented the average of the data and consistently gave similar ranges for the τ_i values. Both τ_1 and τ_2 values for vitrified and frozen samples were significantly lower than for fresh samples, indicating faster relaxation. While the average values of Young's modulus appeared to decrease with freezing and vitrification, this was not found to be statistically significant. This altered stress-relaxation behavior following freezing is, again, partially supported by the work of other groups. Black et al. found that the relaxed shear modulus of previously frozen cartilage was reduced relative to cartilage stored for 10 days (itself reduced relative to fresh tissue) and that retardation times were increased.³² The aggregate modulus and the half-life of stress relaxation were determined using confined compression of porcine femoral cartilage in a study by Willett et al. and both were found to decrease after a freeze-thaw cycle.¹⁵

The altered time constants are evidence of increased permeability of the ECM. In the case of frozen samples this may be a result of ice formation disrupting or damaging the solid phase matrix such that porosity is increased and fluid flow is facilitated, as previously proposed by others.¹⁵ While some partial ice formation cannot be ruled out in the case of vitrified samples, it is unlikely considering the CPA concentrations were sufficiently high to achieve vitrification (8 M). Jomha et al. demonstrated that a DMSO concentration of 6 M or more permitted complete vitrification, absence of ice, and minimal matrix disruption.²⁷ Our hypothesis that vitrification would protect against mechanical alterations was premised primarily on the avoidance of matrix disruption resultant from ice formation. That there were mechanical alterations in the stress-relaxation response post-vitrification, requires explanation. The osmotic stress of vitrification (repeated swelling and shrinking), which results from exposure to CPA solutions of different osmolalities, could adversely alter matrix structure and composition.¹¹ For example, if stress secondary to osmotic flow was sufficient to fragment proteoglycans or the collagen network, matrix permeability could increase and manifest as a shorter relaxation time, as seen here. The osmotic pressure within the ECM has been shown to be primarily due to excess ions attracted to the fixed negative groups

of glycosaminoglycans.³³ If, for instance, the highly polar S=O group of DMSO³⁴ were to draw ions out of the ECM during CPA loading and these were not replaced by ions circulating in the DMEM, this mechanism may also have limited the osmotic pressure resisting fluid exudation. Another possibility is the rapid flow of water out of the matrix upon initial exposure to the high concentration of CPAs (without intervening sequential increases in CPA concentrations to manage the flow) may have caused physical damage to the matrix components. To confirm an explanation for both frozen and vitrified groups will necessitate further research. It should be noted that the decrease in relaxation time constants between the groups represents a small difference that may only become apparent with constant, prolonged loading, as opposed to the more rapid cyclic loading of normal walking. The actual impact of these differences in behavior will be investigated with a transplant study in future work.

From a clinical perspective, these results raise questions, to be expected for a pilot study. The majority of the mechanical results for both frozen and vitrified grafts were not different from the fresh grafts, but Pallante et al.⁸ has shown that frozen grafts deteriorate over 6 months after transplantation due to matrix disorganization. It is known that frozen grafts do not have live chondrocytes to restore graft integrity, which could be possible in the vitrified grafts. Further, the fresh and frozen conditions used in this study do not mimic clinical practice. The clinical standard for “fresh” would be after storage for 21–28 days at 4°C in some maintenance media as compared to the 40 h of storage here. The frozen grafts clinically are typically frozen at approximately 1°C per minute compared to rapid immersion in LN₂ in this study which is approximately 60°C per minute.³⁵ Slow freezing causes much larger ice crystal formation which can impart larger structural damage on the cartilage matrix than smaller ice crystals from rapid freezing. Thus, the mechanical differences noted here may not be equivalent to those that cause graft deterioration in other published clinical studies and it is difficult to know whether the one difference noted in this study has clinical implications. Testing a fourth group of experimental samples, prepared by slow freezing and thawing cycles, was not included within the study but would be beneficial to assess in future study designs. The intent of this study was not to closely mimic clinical storage protocols, but instead to act as a first step in evaluating mechanical differences between storage methods generally. For this reason, experimentally simple methods of freezing and vitrification were employed. Future studies will continue with investigations designed to address some of these clinical questions.

The present study investigated the changes in mechanical properties of the AC tissue under rapid loading and stress-relaxation with vitrification and

freezing compared to fresh tissue. It was found that both freezing and vitrification maintain the mechanical integrity of AC under rapid loading and at equilibrium conditions, but may result in faster stress-relaxation compared to fresh tissue. Thus, our hypothesis was only partially correct and, as such, next steps will include investigation of the effect of osmotic stress and water movement on ECM properties during vitrification and more closely reflect clinical practice. Optimization of the vitrification protocol may improve the results. Performing histology after mechanical testing would also be of value to assess the effect of testing on the cellular and extracellular components of the samples, keeping in mind that long mechanical testing may alter the histology of the samples. Furthermore, the clinical significance of this difference in stress-relaxation behavior between fresh and vitrified AC requires exploration with transplantation studies. To our knowledge, this is the first study that endeavors to compare the mechanical properties of fresh, frozen and vitrified AC.


Declaration of conflicting interests

The author(s) declared no potential conflicts of interest with respect to the research, authorship, and/or publication of this article.

Funding

The author(s) disclosed receipt of the following financial support for the research, authorship, and/or publication of this article: This work was supported by the Edmonton Orthopaedic Research Committee. J.H. is funded by the Alberta Innovates Summer Research Studentship (SRS). I.W. is funded by the Natural Sciences and Engineering Research Council (NSERC). K.W. is funded by the Li Ka Shing Sino-Canadian Exchange Program between University of Alberta and Shantou University. Samples were obtained from Delton Sausage & Deli in Edmonton, Alberta.

ORCID iD

Lindsey Westover  <https://orcid.org/0000-0003-1220-3967>

References

1. Chahla J, Dean CS, Moatshe G, et al. Concentrated bone marrow aspirate for the treatment of chondral injuries and osteoarthritis of the knee: a systematic review of outcomes. *Orthop J Sports Med* 2016; 4: 2325967115625481.
2. Bugbee WD, Pallante-Kichura AL, Görtz S, et al. Osteochondral allograft transplantation in cartilage repair: graft storage paradigm, translational models, and clinical applications. *J Orthop Res* 2016; 34: 31–38.
3. Torrie AM, Kesler WW, Elkin J, et al. Osteochondral allograft. *Curr Rev Musculoskelet Med* 2015; 8: 413–422.

4. Williams SK, Amiel D, Ball ST, et al. Analysis of cartilage tissue on a cellular level in fresh osteochondral allograft retrievals. *Am J Sports Med* 2007; 35: 2022–2032.
5. Raz G, Safir OA, Backstein DJ, et al. Distal femoral fresh osteochondral allografts: follow-up at a mean of twenty-two years. *J Bone Joint Surg Am* 2014; 96: 1101–1107.
6. Mickevicius T, Pockevicius A, Kucinskas A, et al. Impact of storage conditions on electromechanical, histological and histochemical properties of osteochondral allografts. *BMC Musculoskelet Disord* 2015; 16: 314.
7. Williams RJ, Dreese JC and Chen CT. Chondrocyte survival and material properties of hypothermally stored cartilage: an evaluation of tissue used for osteochondral allograft transplantation. *Am J Sports Med* 2004; 32: 132–139.
8. Pallante AL, Görtz S, Chen AC, et al. Treatment of articular cartilage defects in the goat with frozen versus fresh osteochondral allografts: effects on cartilage stiffness, zonal composition, and structure at six months. *J Bone Joint Surg Am* 2012; 94: 1984–1995.
9. Brockbank KG, Chen ZZ and Song YC. Vitrification of porcine articular cartilage. *Cryobiology* 2010; 60: 217–221.
10. Jomha NM, Elliott JA, Law GK, et al. Vitrification of intact human articular cartilage. *Biomaterials* 2012; 33: 6061–6068.
11. Abazari A, Jomha NM, Elliott JA, et al. Cryopreservation of articular cartilage. *Cryobiology* 2013; 66: 201–209.
12. Szarko M, Muldrew K and Bertram JE. Freeze-thaw treatment effects on the dynamic mechanical properties of articular cartilage. *BMC Musculoskelet Disord* 2010; 11: 231.
13. Muldrew K, Hurtig M, Novak K, et al. Localization of freezing injury in articular cartilage. *Cryobiology* 1994; 31: 31–38.
14. Muldrew K, Novak K, Yang H, et al. Cryobiology of articular cartilage: ice morphology and recovery of chondrocytes. *Cryobiology* 2000; 40: 102–109.
15. Willett TL, Whiteside R, Wild PM, et al. Artefacts in the mechanical characterization of porcine articular cartilage due to freezing. *Proc IMechE, Part H: J Engineering in Medicine* 2005; 219: 23–29.
16. Kennedy EA, Tordonado DS and Duma SM. Effects of freezing on the mechanical properties of articular cartilage. *Biomed Sci Instrum* 2007; 43: 342–347.
17. Wu K, Laouar L, Shardt N, et al. Comparison of three multi-cryoprotectant loading protocols for vitrification of articular cartilage. *Cryobiology* 2018; 85: 153.
18. Ateshian GA, Ellis BJ and Weiss JA. Equivalence between short-time biphasic and incompressible elastic material responses. *J Biomech Eng* 2007; 129: 405–412.
19. Brown CP, Nguyen TC, Moody HR, et al. Assessment of common hyperelastic constitutive equations for describing normal and osteoarthritic articular cartilage. *Proc IMechE, Part H: J Engineering in Medicine* 2009; 223: 643–652.
20. Andrews SH, Rattner JB, Shrive NG, et al. Swelling significantly affects the material properties of the menisci in compression. *J Biomech* 2015; 48: 1485–1489.
21. Fernández P, Lamela Rey MJ and Fernández Canteli A. Viscoelastic characterisation of the temporomandibular joint disc in bovines. *Strain* 2011; 47: 188–193.
22. Korhonen RK, Laasanen MS, Töyräs J, et al. Comparison of the equilibrium response of articular cartilage in unconfined compression, confined compression and indentation. *J Biomech* 2002; 35: 903–909.
23. Mow VC, Kuei SC, Lai WM, et al. Biphasic creep and stress relaxation of articular cartilage in compression? Theory and experiments. *J Biomech Eng* 1980; 102: 73–84.
24. Judas F, Rosa S, Teixeira L, et al. Chondrocyte viability in fresh and frozen large human osteochondral allografts: effect of cryoprotective agents. *Transplant Proc* 2007; 39: 2531–2534.
25. Ohlendorf C, Tomford WW and Mankin HJ. Chondrocyte survival in cryopreserved osteochondral articular cartilage. *J Orthop Res* 1996; 14: 413–416.
26. Zheng S, Xia Y, Bidthanapally A, et al. Damages to the extracellular matrix in articular cartilage due to cryopreservation by microscopic magnetic resonance imaging and biochemistry. *Magn Reson Imaging* 2009; 27: 648–655.
27. Jomha NM, Anoop PC and McGann LE. Intramatrix events during cryopreservation of porcine articular cartilage using rapid cooling. *J Orthop Res* 2004; 22: 152–157.
28. Boschetti F, Pennati G, Gervaso F, et al. Biomechanical properties of human articular cartilage under compressive loads. *Biorheology* 2004; 41: 159–166.
29. Henak CR, Kapron AL, Anderson AE, et al. Specimen-specific predictions of contact stress under physiological loading in the human hip: Validation and sensitivity studies. *Biomech Model Mechanobiol* 2014; 13: 387–400.
30. Changoor A, Fereydoonzad L, Yaroshinsky A, et al. Effects of refrigeration and freezing on the electromechanical and biomechanical properties of articular cartilage. *J Biomech Eng* 2010; 132: 064502.
31. Lee H, Campbell WD, Theis KM, et al. Comparison between the hyperelastic behavior of fresh and frozen equine articular cartilage in various joints. *J Biomech Eng* 2020; 142: 0245011–0245016.
32. Black J, Shadle CA, Parsons JR, et al. Articular cartilage preservation and storage. II. Mechanical indentation testing of viable, stored articular cartilage. *Arthritis Rheum* 1979; 22: 1102–1108.
33. Maraudas A. Proteoglycan osmotic pressure and the collagen tension in normal, osteoarthritic human cartilage. *Semin Arthritis Rheum* 1981; 11: 36–39.
34. Weng L, Stott SL and Toner M. Exploring dynamics and structure of biomolecules, cryoprotectants, and water using molecular dynamics simulations: Implications for biostabilization and biopreservation. *Annu Rev Biomed Eng* 2019; 21(1): 1–31.
35. Jomha NM, Anoop PC, Bagnall K, et al. Effects of increasing concentrations of dimethyl sulfoxide during cryopreservation of porcine articular cartilage. *Cell Preserv Technol* 2002; 1: 111–120.